

Different polarization definitions in same-sign WW scattering at the LHC.

Alessandro Ballestrero^a, Ezio Maina^{a,b}, Giovanni Pelliccioli^c

^a*INFN, Sezione di Torino, via Pietro Giuria 1, 10125 Torino (Italy)*

^b*University of Torino, Department of Physics, via Pietro Giuria 1, 10125 Torino (Italy)*

^c*University of Würzburg, Institut für Theoretische Physik und Astrophysik, Emil-Hilb-Weg 22, 97074 Würzburg (Germany)*

Abstract

We study the polarization of positively charged W 's in the scattering of massive electroweak bosons at hadron colliders. We rely on the separation of weak boson polarizations in the gauge-invariant, doubly-resonant part of the amplitude in Monte Carlo simulations. Polarizations depend on the reference frame in which they are defined. We discuss the change in polarization fractions and in kinematic distributions arising from defining polarization vectors in two different reference frames which have been employed in recent experimental analyses.

Keywords: Vector Boson Scattering, LHC, Polarization, Electroweak

1. Introduction

Vector Boson Scattering (VBS) at the LHC represents a crucial process for both Standard Model (SM) analyses and for Beyond-the-Standard-Model (BSM) searches. The $W^\pm W^\pm$ channel with leptonic decays features the largest signal-to-background ratio among VBS processes. It has been measured [1–4] and studied [5–8] in LHC proton-proton collisions with $\sqrt{s} = 8$ and 13 TeV, and the luminosity increase expected for the next runs will yield more accurate measurements [9–11].

A detailed study of VBS with two positively-charged leptons and missing transverse momentum in the final state is presented in Ref. [12]. Predictions include NLO QCD corrections and are matched to parton showers.

The importance of VBS with longitudinal bosons is related to the delicate cancellation of large, unitarity-violating contributions in the SM, that come respectively from pure gauge and from Higgs diagrams. Any modification of the SM realization of the Electroweak Symmetry Breaking mechanism (EWSB) could interfere with this delicate cancellations in VBS. Therefore, it is essential to devise a good definition of polarized signals at the theoretical level, and to investigate their phenomenology, in order to identify observables which allow the efficient experimental separation of polarized processes at the LHC.

Both CMS and ATLAS have measured the W polarization fractions in the W +jets [13, 14] channel and in $t\bar{t}$ events [15–17]. Z polarization fractions at the LHC have been measured in [18, 19]. The first polarization measurement at 13 TeV has been performed by ATLAS in WZ production [20].

In Refs. [21, 22] we extensively investigated the W^+W^- , W^+Z and ZZ scattering channels. In the fully-leptonic W^+W^+ scattering, like in W^+W^- , the presence of two neutrinos in the final state inhibits the experimental reconstruction of the center-of-mass frame of each W boson. This strongly limits the search for kinematic variables which are sensitive to vector boson polarizations. A more in-depth understanding of the polarization structure of W^+W^+ is urgent. Although a number of results are reported in Ref. [23, 24], a detailed study of same sign W 's scattering, in the spirit of Refs. [21, 22], is still missing.

The predictions presented here are not fully realistic, since we are considering only the leading order SM electroweak signal for VBS, without including the QCD background, higher-order corrections and parton-shower effects. This paper could serve as a benchmark study in view of more precise investigations.

Two are the novel features with respect to Refs. [21, 22]. First, we focus on doubly-polarized distributions; second, we investigate the effect of defining the polarization vectors in different reference frames. We are further motivated by the fact that the experimental analyses in Refs. [13–20] employ distinct definitions of polarizations.

The paper is organized as follows. In Sect. 2 we recall quickly the theoretical concepts which are needed to separate polarization modes of weak bosons in a VBS context. After describing the setup of our simulations in Sect. 3, and showing a few results in the absence of lepton cuts in Sect. 4, we present integrated cross-sections and relevant distributions for polarized W bosons in the presence of realistic lepton cuts (Sect. 5). We focus on observables with discriminating power among different polarization modes, and on the shift in polarization fractions arising from defining polarization vectors in two different reference frames. In Sect. 6 we briefly address the effect due

Email addresses: ballestr@to.infn.it (Alessandro Ballestrero), maina@to.infn.it (Ezio Maina), giovanni.pelliccioli@physik.uni-wuerzburg.de (Giovanni Pelliccioli)

to different polarization vector definitions in other VBS channels (W^+W^- , W^+Z and ZZ), limiting ourselves to integrated cross-sections. Finally, in Sec. 7 we draw our conclusions.

2. Defining polarized signals at the LHC

Electroweak massive bosons feature three physical polarization modes, longitudinal, left- and right-handed. The production of a boson with definite polarization state is well-defined only for an on-shell boson. However, being unstable particles, W 's and Z 's decay into leptons or quarks before detection. A possible solution is to split the numerator of a W/Z boson propagator into a sum of terms, one for each physical polarization state: this statement holds for a general ξ -gauge choice, if weak boson decay products are massless. Selecting a single term in the sum, corresponds to selecting a definite polarization state of the propagating boson.

An additional complication is the non-resonant character of many diagrams in multi-boson processes already at tree-level. For W^+W^+ scattering at the LHC, doubly-resonant, singly-resonant and non-resonant diagrams contribute at $\mathcal{O}(\alpha^6)$. The latter two classes of diagrams don't expose a factorized structure (production \times propagator \times decay), therefore for them separating polarized terms is simply impossible. An approximate solution to this problem is to consider doubly-resonant diagrams only, and treating them with a double-pole approximation [25] to recover $SU(2)_L \times U(1)_Y$ gauge invariance. More specifically we employ the same on-shell projection technique (OSP) introduced for W^+W^- in Ref. [21].

For the aim of this paper, it is essential to recall that the definition of polarizations is not unique, since polarization vectors are not Lorentz covariant. For a boson with momentum p and polarization state λ , and a generic Lorentz transformation Λ , it can be proved that $\varepsilon_\lambda^\mu(\Lambda \cdot p) \neq \Lambda^\mu_\nu \varepsilon_\lambda^\nu(p)$. Therefore, we need to specify the reference frame in which polarization vectors are computed. In Refs. [21, 22], they are defined in the laboratory, which is a natural choice at the LHC. Recently, the ATLAS Collaboration measured polarizations in WZ -pair production [20], defining polarization observables in the boson-boson center-of-mass frame. This choice has the advantage that the lines of flight of the two bosons, whose direction determines the longitudinal polarization vectors, are equal, up to a change of sign. It is also more directly related to the weak boson scattering process embedded in the hadronic process and therefore, it might be better suited to the search for new physics affecting the EWSB mechanism. Phenomenological studies with polarization vectors defined in the boson-boson center-of-mass have recently appeared [26].

In the following we discuss singly- and doubly-polarized integrated cross-sections and distributions, comparing the results with polarization vectors defined in:

- the laboratory frame (Lab);

- the center-of-mass frame of the two W^+ bosons (WW CoM),

focusing on how the two different definitions affect the distributions of kinematic variables that are observable at the LHC.

The possibility of defining the polarization vectors in the Lab or in the WW CoM has been recently introduced in PHANTOM [27]. Different reference frames to define polarizations are available in MADGRAPH5 [28].

3. Setup

The process under investigation is $pp \rightarrow jj e^+ \nu_e \mu^+ \nu_\mu$ with center-of-mass energy of 13 TeV. All the total cross-sections and distributions shown below have been computed at parton-level with the PHANTOM [27] Monte Carlo, using NNPDF3.0 PDFs [29] computed at LO. The factorization scale is set to $\mu_F = (p_t^{j1} p_t^{j2})^{1/2}$. We only consider leading-order pure electroweak contributions, $\mathcal{O}(\alpha^6)$, which are usually considered as the VBS signal, in contrast with the QCD background ($\mathcal{O}(\alpha^4 \alpha_s^2)$). We employ the Complex-Mass Scheme [30, 31] for SM couplings and masses in full computations, while the OSP results rely on real couplings with vanishing weak boson widths (apart from the widths appearing in the off-shell propagators denominators corresponding to projected W^+ 's). We use the following pole masses and widths for weak bosons: $M_W = 80.358$ GeV, $M_Z = 91.153$ GeV, $\Gamma_W = 2.084$ GeV, $\Gamma_Z = 2.494$ GeV. The Fermi constant is set to $G_\mu = 1.16637 \cdot 10^{-5}$ GeV $^{-2}$.

The following selection cuts are understood for all results:

- maximum jet pseudorapidity, $|\eta_j| < 5$;
- minimum jet transverse momentum, $p_t^j > 20$ GeV;
- minimum jet-jet invariant mass, $M_{jj} > 500$ GeV;
- minimum jet-jet pseudorapidity separation, $|\Delta\eta_{jj}| > 2.5$.

These selections define the inclusive setup, which is considered in Sect. 4. In Sect. 5, three additional cuts are applied to the simulated events:

- maximum lepton pseudorapidity, $|\eta_\ell| < 2.5$;
- minimum lepton transverse momentum, $p_t^\ell > 20$ GeV;
- minimum missing transverse momentum, $p_t^{\text{miss}} > 40$ GeV.

Applying OSP requires the mass of the four lepton system to be larger than twice the W pole-mass, otherwise the technique is not defined. It is worth noting that the number of events below this threshold is roughly 0.6% in the full calculation. This means that comparing full results computed over the whole range of $M_{4\ell}$ and OSP results (polarized and unpolarized) computed for $M_{4\ell} > 161$ GeV does not introduce any relevant bias. This is the procedure adopted in the following.

4. Validation in the absence of lepton cuts

In this section we concentrate on the inclusive setup, as defined above. These results, without selection cuts on leptons, are not realistic, but useful to understand the quality of the signal definition and to get a first feeling of the polarization structure in the scattering process.

In Tab. 1 we show the total cross-sections for the unpolarized, singly-polarized and doubly-polarized signal, with the two polarization definitions (in the Lab and in the WW CoM). As a first comment the unpolarized OSP result re-

	Lab	WW CoM	ratio
full	3.185(3)		-
unpol	3.167(2)		-
0-unpol	0.8772(8)	0.8374(9)	0.95
T-unpol	2.287(2)	2.329(2)	1.02
0-0	0.2573(3)	0.3275(4)	1.27
0-T, T-0	0.6199(6)	0.5081(5)	0.82
T-T	1.666(1)	1.820(1)	1.09

Table 1: Total cross-sections (fb) for W^+W^+ scattering in the absence of lepton cuts. In the first column “0” stands for longitudinal, “T” for transverse, “unpol” for unpolarized. The first label is relative to the W^+ that decays into $e^+\nu_e$, the second one to the W^+ decaying into $\mu^+\nu_\mu$. The ratios are computed as polarized results in the WW CoM over those in the Lab. Number in parentheses are numerical MC errors.

produces at the sub-percent level the full cross-section. The good behavior of the OSP approximation is further confirmed at the differential level in most of the distributions we have considered.

The singly-polarized cross-sections are similar to each other in the two definitions. The longitudinal one decreases by 5% passing from the Lab to the WW CoM, while the transverse one increases by 2%. Note that the sum of longitudinal and transverse polarizations approximates the unpolarized result to better than 1% with both definitions. The longitudinal fraction is 28% of the total in the Lab, 26% in the WW CoM.

The differences between the polarization fractions computed in the two reference frames are larger for the doubly-polarized results. In the WW CoM, the longitudinal-longitudinal and transverse-transverse cross-sections are 27% and 9% larger, respectively, with respect to the corresponding ones in the Lab, while the mixed contributions are 18% smaller. Therefore, the WW CoM definition might be more useful in extracting the longitudinal-longitudinal contribution from the unpolarized process.

Given the large number of final state particles, one could naïvely expect that the doubly-polarized fractions could be obtained as products of singly-polarized ones. This would be true if the two boson spin states were not correlated. In the Lab, this would give a longitudinal-longitudinal cross-section of 0.24 fb which is not so far from the Monte Carlo result (0.26 fb). The mixed contributions would both be

0.64 fb, and the doubly-transverse 1.67 fb, to be compared with the actual values 0.62 fb and 1.67 fb, respectively. In the Lab, the correlation between the two bosons polarizations is mild, and its effect is hardly visible in configurations which involve transverse bosons.

The correlation is much more evident in the WW CoM. Under the zero-correlation hypothesis, the doubly-longitudinal rate would amount to 0.22 fb, which is 35% lower than the value computed by the Monte Carlo.

We have tested the validity of the polarized signals comparing Monte Carlo results with those extracted analytically from the angular distributions of the decay leptons. Using the analytic expression for the W^+ LO differential decay rate in the lepton angle θ_ℓ^* (computed in the W rest frame),

$$\frac{1}{\sigma} \frac{d\sigma}{d\cos\theta_{\ell^+}^*} = \frac{3}{4} f_0 \sin^2\theta_{\ell^+}^* + \frac{3}{8} f_L (1 - \cos\theta_{\ell^+}^*)^2 + \frac{3}{8} f_R (1 + \cos\theta_{\ell^+}^*)^2, \quad (1)$$

one can easily extract the polarization fractions f_0, f_L, f_R projecting the unpolarized $\cos\theta_{\ell^+}^*$ distribution onto the first three Legendre polynomials [21]. If the polarizations are defined in the Lab (WW CoM), $\theta_{\ell^+}^*$ must be computed with respect to the W^+ direction in the Lab (WW CoM) frame.

Note that this method can be applied to extract single polarization fractions from the full distribution as well as to extract double polarization fractions from singly-polarized distributions. We have performed all these checks, for both polarization definitions, finding perfect agreement with the distributions computed directly with the Monte Carlo, both in normalization and in shape. As a last comment, we stress that most differential distributions are strongly similar in the two polarization definitions. However, there are kinematic observables, like the charged lepton pseudorapidity, for which the distributions are noticeably different. We will return to this point in the next section.

5. Results with lepton cuts

Imposing cuts on leptons is unavoidable at the LHC. Therefore, for our purposes, it is essential to study the kinematic distributions for polarized intermediate W bosons in the presence of transverse momentum and pseudorapidity cuts on the final state leptons, to address the extraction of polarization fractions and polarized cross-sections in a realistic setup. In this section, the complete set of selection cuts described in Sect. 3 is applied.

In analogy with Sect. 4, we start by presenting in Tab. 2 the total cross-sections for singly- and doubly-polarized VBS signals. It is well known [21, 32, 33] that lepton cuts spoil the cancellation of interference terms between different polarization modes. In fact, the sum of singly- or doubly-polarized cross-sections is roughly 1.5%

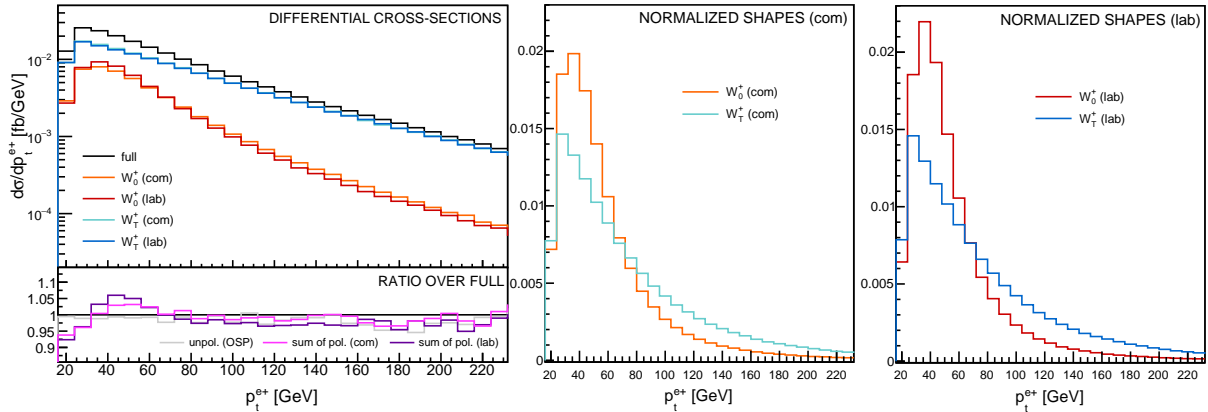


Figure 1: Distributions in the positron transverse momentum, in the presence of lepton cuts. The W^+ decaying into $e^+\nu_e$ has definite polarization state, while the one decaying into $\mu^+\nu_\mu$ is unpolarized. The polarizations are defined in the CoM frame of the WW system (com) or in the laboratory frame (lab). The figure is organized as follows: differential distributions (top left), ratio over the full result (bottom left), distribution shapes normalized to have unit integral for polarized signals defined in the WW CoM (middle) and in the Lab (right).

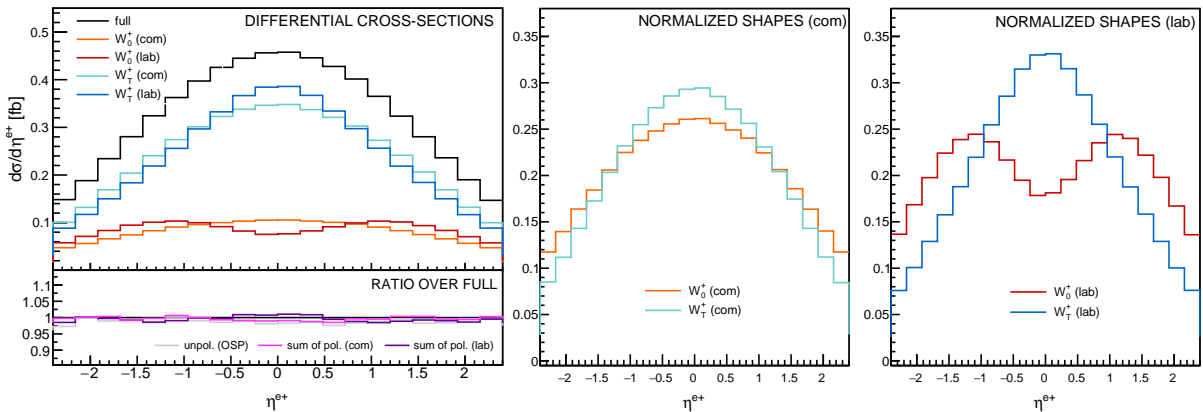


Figure 2: Distributions in the positron pseudorapidity, in the presence of lepton cuts. The figure is structured as Fig. 1.

	Lab	WW CoM	ratio
full	1.593(2)		-
unpol	1.572(2)		-
0-unpol	0.4226(4)	0.4036(5)	0.96
T-unpol	1.165(1)	1.182(2)	1.01
0-0	0.1185(1)	0.1552(2)	1.31
0-T,T-0	0.3062(3)	0.2519(3)	0.82
T-T	0.8690(9)	0.9350(9)	1.08

Table 2: Total cross-sections (fb) or W^+W^+ scattering in the presence of lepton cuts. Same notation as in Tab. 1.

larger than the OSP unpolarized one, signaling small negative interferences. The off-shell effects that are missing in the OSP approximation are of the same order of magnitude but positive. This results in a sum of polarized signals which reproduces to less than 0.5% the full cross-section. Applying lepton cuts reduces all cross-sections by roughly a factor of two, but does not sizeably

change the polarization fractions obtained in the inclusive setup. The differences between the two polarization definitions are essentially unchanged, apart from a mild enhancement in the longitudinal-longitudinal contribution in the WW CoM definition (+31%, w.r.t. the Lab). The doubly-longitudinal fraction is 7.5%(10%), while the doubly-transverse cross-section is the dominant one, as expected, accounting for the 55%(59%) of the total in the Lab(WW CoM). Each of the two mixed contributions accounts for the remaining 19%(16%).

As already observed in the inclusive case, the singly-polarized signals are rather insensitive to the polarization definition. The singly-longitudinal(transverse) fraction accounts for the 26%(70%) of the total, in both definitions.

Since both are experimentally interesting, in the following we present singly- and doubly-polarized differential distributions for some relevant variables.

Kinematic observables which depend on the decay products of a single W are natural choices for the extraction of the polarized components of a single boson.

In Fig. 1 we consider the transverse momentum of the

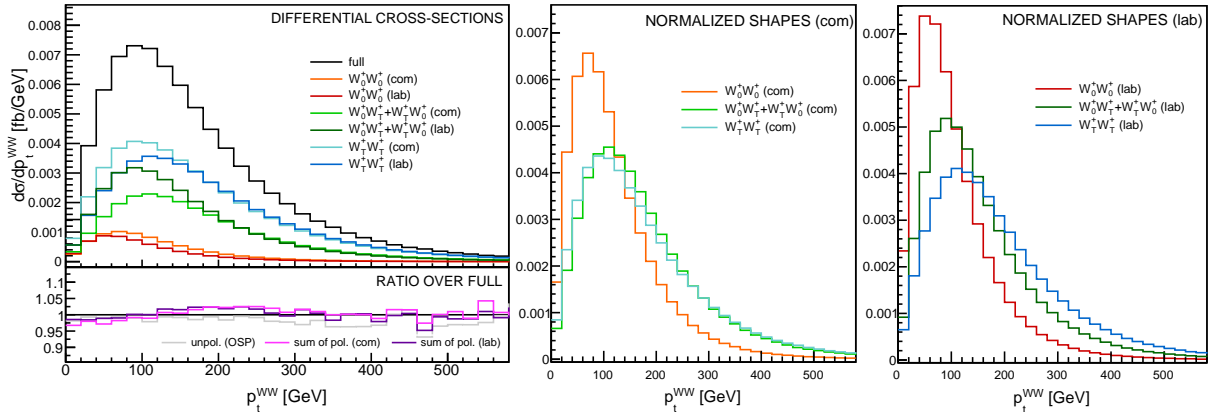


Figure 3: Distributions in the four lepton system transverse momentum, in the presence of lepton cuts. Both W^+ bosons have definite polarization state. The polarizations are defined in the CoM frame of the WW system (com) or in the laboratory frame (lab). The figure is organized as follows: differential distributions (top left), ratio over the full result (bottom left), distribution shapes normalized to unit integral for polarized signals defined in the WW CoM (middle) and in the Lab (right).

positron. These distributions confirm that the differences between the two polarization definitions are very small, particularly for the transverse component, for which even the normalized shapes are almost identical. The longitudinal component shows a 4% discrepancy at the integrated level. The shapes are also different: the distribution in the Lab is slightly narrower around the peak at 35 GeV.

The distribution of the positron transverse momentum for longitudinal and transverse polarization are significantly different. The former has a large peak around 35 GeV, while the latter is harder, with a smaller peak close to the threshold at 20 GeV.

The interferences are generally small, reaching 5-6% in the soft region of the spectrum. They change sign at about 30 GeV. The OSP description of the unpolarized process is good, even in the tail of the distribution.

The positron pseudorapidity is shown in Fig. 2. The OSP technique performs very well, and the interferences are below 2% in the whole range $|\eta_e| < 2.5$. Although the integrated cross-section for singly-polarized configurations gives similar results in the two definitions, there are relevant differences in the distributions. In the WW CoM, the longitudinal and transverse distributions feature a maximum at zero pseudorapidity. The transverse shape is narrower. On the contrary, in the Lab, the two polarization modes are quite distinct. The transverse distribution is similar to the WW CoM one, while the longitudinal has two peaks for $|\eta_{e^+}| \approx 1$ and a local minimum at zero pseudorapidity. In this case it is clearly easier to separate the longitudinal from the transverse component if the polarizations are defined in the Lab. The positron pseudorapidity is the first evidence that different polarization definitions can give very different results for some kinematic variables, even if the polarization fractions are similar. Therefore a detailed comparison of the full set of experimental observables with different polarization definitions should be performed.

We now move to doubly-polarized distributions, in order to gain a more detailed understanding of the spin structure of same sign off-shell W bosons produced in VBS at the LHC.

In the following we present the differential cross-sections for two observables that depend on the charged lepton and neutrino kinematics, and that are symmetric under the exchange of the two lepton flavours. This means that the longitudinal-transverse and transverse-longitudinal distributions are equal. Therefore, we sum them in a single mixed polarization result.

In Fig. 3 we consider the vector sum of the charged leptons transverse momenta and of the missing transverse momentum, which is accessible at the LHC. Since there is no explicit cut on this variable, it might be better suited for the study of the shapes of distributions with the purpose of discriminating among polarization states. This observable is very well described by the doubly resonant OSP unpolarized calculation, as the discrepancies with respect to the full distribution amount at a few percent in all parts of the spectrum. The interferences are almost negligible in the soft region, small, less than 5%, and negative for $p_t^{WW} > 150$ GeV. The transverse and mixed distributions in the WW CoM differ considerably from the ones in the Lab, mostly in the region around the peak. In this range, the noticeable enhancement of the doubly-transverse component in the WW CoM is counterbalanced by the reduction of the mixed ones. On the contrary, a sizeable enhancement of the doubly-longitudinal component in the WW CoM arises above the peak, for $p_t^{WW} > 60$ GeV. In the WW CoM, the distribution shapes for the doubly-transverse and mixed contributions are quite similar, and feature a peak at $p_t^{WW} \approx 100$ GeV. In the Lab, the mixed polarization distribution is narrower than the doubly-transverse one. In both polarization definitions, the longitudinal-longitudinal distribution peaks at lower values than the other components, for

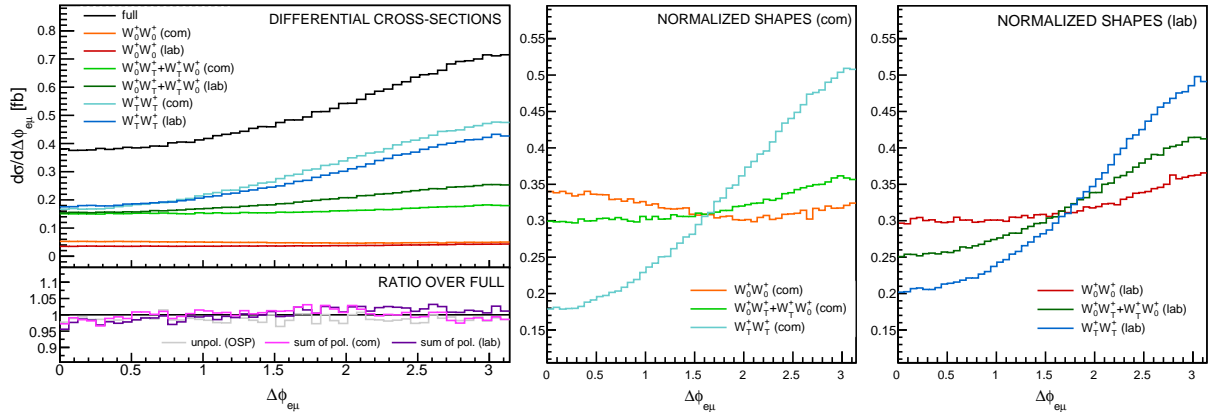


Figure 4: Distributions in the azimuthal separation between the two charged leptons, in the presence of lepton cuts. The figure is structured as Fig. 3.

$p_t^{WW} \approx 70(80)$ GeV in the Lab (WW CoM).

It should be mentioned that, at LO, the four-lepton system transverse momentum coincides with the transverse momentum of the two tagging jets. Therefore, this variable is expected to be sensitive to additional QCD radiation.

The marked shape differences among the doubly-polarized states, the small interferences and the good OSP description make this observable well suited for extracting polarizations, provided higher-order perturbative corrections, parton-shower and detector effects do not disrupt too much the distribution shapes.

In the last part of this section we consider the azimuthal separation between the two charged leptons $\Delta\phi_{e\mu}$. This angular variable is expected to be measured with high accuracy at the LHC. In Fig. 4 we show the doubly-polarized distributions. Interferences among polarizations and non-resonant effects never exceed 4%. Even though interference terms are small, in our experience [21, 22], it is useful to include them in fitting the data with polarized distributions. Note that large interferences in $\Delta\phi$ can arise in other processes [34, 35].

The unpolarized distributions and those involving at least one transverse boson, peak at $\Delta\phi_{e\mu} = \pi$. The doubly-longitudinal component is flatter in both polarization definitions. The mixed contribution is rather flat in the WW CoM, while in the Lab its shape is intermediate between the longitudinal and the transverse components. All the polarized distributions are approximately symmetric about $\Delta\phi_{e\mu} = \pi/2$. However, the shapes are noticeably different for the three doubly-polarized states, particularly in the WW CoM. Despite a lower discrimination power, the sensitivity of $\Delta\phi_{e\mu}$ to the different polarization states is evident even in the Lab.

We have examined a number of other kinematic observables. They are not presented here because they have less discriminating power than the variables we have shown above. As an example, we have examined the R_{p_t} variable

proposed in Ref. [36] to improve the sensitivity to new physics effects. We found that the shape of the R_{p_t} distribution is roughly the same for longitudinal and transverse W bosons.

We only investigated a limited number of observables, one at a time, at parton level. A more comprehensive and realistic study is clearly warranted in order to optimize the multi-variate analysis of available data.

6. A quick review of other VBS processes.

Even though this work focuses on the scattering of two same sign W bosons, it is interesting to investigate whether the two different polarization definitions give different results also in the other vector boson scattering processes at the LHC. All the results of Refs. [21, 22] have been obtained with polarization vectors defined in the Lab. In this section we present polarized total cross-sections for the following processes:

- $pp \rightarrow jj e^+ \nu_e \mu^- \bar{\nu}_\mu$ ($W^+ W^-$);
- $pp \rightarrow jj e^+ \nu_e \mu^+ \mu^-$ ($W^+ Z$);
- $pp \rightarrow jj e^+ e^- \mu^+ \mu^-$ (ZZ).

We have simulated $W^+ W^-$ scattering using the inclusive setup described in Sect. 3. Since the OSP results (polarized and unpolarized) are naturally restricted to the region $M_{WW} > 2M_W$, we have applied the same cut to the full calculation. This excludes the contribution of s -channel Higgs production and allows a meaningful comparison between the two results. While a direct cut on the mass of the WW system is unrealistic, the Higgs signal can be excluded by appropriate cuts on the leptonic system and the missing momentum. The OSP calculation reproduces the full one very accurately.

In Tab. 3 we show the polarized and unpolarized total cross-sections for opposite-sign W scattering.

	Lab	WW CoM	ratio
full	4.651(2)		-
unpol	4.641(2)		-
0-unpol	1.186(1)	1.146(1)	0.97
T-unpol	3.456(2)	3.494(2)	1.01
unpol-0	1.2226(4)	1.1905(5)	0.97
unpol-T	3.418(1)	3.450(1)	1.01
0-0	0.3314(2)	0.3786(3)	1.14
0-T	0.8545(4)	0.7669(3)	0.90
T-0	0.8912(4)	0.8119(4)	0.91
T-T	2.563(1)	2.683(1)	1.05

Table 3: Total cross-sections (fb) for W^+W^- scattering in the absence of lepton cuts, with $M_{4\ell} > 2M_W$ GeV.

The singly-polarized cross-sections are very similar in the two definitions. They differ by about 1% for the transverse case and by 3% for the longitudinal one. These results are in line with those obtained in same-sign WW scattering, suggesting that such effects are not specific to W^+W^+ .

Doubly-polarized signals also show a trend similar to the one for same-sign bosons. The doubly-longitudinal WW CoM signal is 14% larger than the one in the Lab, while the purely transverse is larger by 5%. The mixed signals in the WW CoM are 9% smaller than in the Lab.

Encouraged by the strong similarity of the results obtained for both same-sign and opposite-sign WW scattering, one expects the same effects to appear in other VBS channels. For both W^+Z and ZZ , we impose the jet cuts introduced in Sect. 3, and a minimum invariant mass cut of 200 GeV on the four lepton system. The total cross-sections for ZZ and W^+Z are shown in Tabs. 4 and 5, respectively. For ZZ processes, the differences between the two definitions of polarizations are roughly the same as in W^+W^+ , both for singly-polarized and doubly-polarized total cross-sections, as can be observed comparing Tab. 4 with Tab. 1.

	Lab	ZZ CoM	ratio
full	0.1270(1)		-
unpol	0.1264(1)		-
0-unpol	0.03328(2)	0.03104(2)	0.93
T-unpol	0.09295(5)	0.09511(4)	1.02
0-0	0.00910(1)	0.01087(2)	1.19
0-T, T-0	0.02421(2)	0.02022(2)	0.84
T-T	0.06869(3)	0.07490(4)	1.09

Table 4: Total cross-sections (fb) for ZZ scattering in the absence of lepton cuts, with $M_{4\ell} > 200$ GeV.

A detailed analysis of Tab. 5 reveals new aspects that characterize polarized signals in the W^+Z process. The singly-longitudinal cross-section in the WZ CoM is 5-6%

	Lab	WZ CoM	ratio
full	0.5253(3)		-
unpol	0.5210(3)		-
0-unpol	0.1216(1)	0.1292(1)	1.06
T-unpol	0.3992(2)	0.3918(3)	0.98
unpol-0	0.1370(1)	0.1436(1)	1.05
unpol-T	0.3839(2)	0.3773(2)	0.98
0-0	0.03236(3)	0.03993(5)	1.23
0-T	0.08923(8)	0.08926(8)	1.00
T-0	0.1045(1)	0.1039(1)	0.99
T-T	0.2948(2)	0.2876(2)	0.98

Table 5: Total cross-sections (fb) for W^+Z scattering in the absence of lepton cuts, with $M_{4\ell} > 200$ GeV.

larger than in the Lab, both for the W^+ and for the Z boson. This is balanced by the opposite behavior of the dominant transverse contribution, which is 2% smaller in the WZ CoM. These differences between the WZ CoM and the Lab, though not large, go in the opposite direction with respect to the WW and ZZ processes.

Furthermore, the doubly-longitudinal signal in the WZ CoM is about 20% larger than in the Lab. This enhancement is balanced by the decrease of the transverse-transverse contribution, and not of the mixed ones as in WW processes. The mixed configurations have almost exactly the same cross-section with both definitions ($\lesssim 0.5\%$ differences).

As a last result of this section, we have found that the differences between the two polarizations definitions in same-sign WW are not peculiar to the SM dynamics, but are present even in the strongly interacting Higgsless model (SM with $M_H \rightarrow \infty$). Using the same cuts as in Sect. 4, we have checked numerically that in the Higgsless model, the longitudinal-longitudinal signal is much larger than the SM one, both in the WW CoM and in the Lab (+80%). Such a large deviation is motivated by the unitarity violations that characterize the high-energy regime, but show up even imposing the loosest possible cut on the WW mass ($M_{WW} > 161$ GeV), which is needed for the OSP to provide a good description of the full results.

7. Conclusions

In this paper, we have investigated the phenomenology of polarized vector bosons in W^+W^+ scattering. We have compared the results obtained defining the electroweak boson polarization vectors in the WW CoM and in the Lab reference frames.

The complex structure of VBS processes makes it difficult to explain analytically the differences between the results in the WW CoM and the Lab in terms of resonant matrix-elements and Lorentz transformations. Therefore, only numerical studies, like the one presented in this paper, can provide a detailed picture of the polarization structure

of multi-boson processes, and identify a set of variables which permits, in a given choice of polarization vectors, to separate the vector boson polarization states in the experimental analyses of LHC data.

We have presented total and differential cross-sections for both singly-polarized and doubly-polarized signals. The singly-polarized signals are weakly sensitive to the polarization definition at the integrated level. The transverse component is typically three times larger than the longitudinal one. The distributions for some kinematic variables, like the single lepton transverse momentum and pseudorapidity, depend noticeably on the W polarization and, therefore, can be used to separate the different contributions and determine the polarization fractions.

The longitudinal-longitudinal and transverse-transverse cross-sections are enhanced by defining polarizations in the WW CoM, while mixed configurations are diminished. This might be useful for searches of deviations from the SM description of EWSB. The differences between the distributions for transverse and longitudinal polarizations in the Lab are slightly larger than in the WW CoM.

Our results do not clearly favor either of the reference frames we have examined for the definition of polarization vectors.

Beyond the specific study of same-sign WW scattering, we have also compared the polarized total cross-sections in the two definitions for other VBS channels. We have found strong similarities with W^+W^+ in W^+W^- and ZZ processes, while new features appear in W^+Z .

Acknowledgements

We thank Ansgar Denner and Lucia Di Ciaccio for useful discussions. The authors acknowledge the VBSCan COST Action CA16108. EM is supported by the SPIF INFN project (Precision Studies of Fundamental Interactions), GP is supported by the German Federal Ministry for Education and Research (BMBF) under contract no. 05H18WWCA1.

References

- [1] G. Aad, et al., Evidence for Electroweak Production of $W^\pm W^\pm jj$ in pp Collisions at $\sqrt{s} = 8$ TeV with the ATLAS Detector, *Phys. Rev. Lett.* 113 (14) (2014) 141803. [arXiv:1405.6241](#), [doi:10.1103/PhysRevLett.113.141803](#).
- [2] A. M. Sirunyan, et al., Observation of electroweak production of same-sign W boson pairs in the two jet and two same-sign lepton final state in proton-proton collisions at $\sqrt{s} = 13$ TeV, *Phys. Rev. Lett.* 120 (8) (2018) 081801. [arXiv:1709.05822](#), [doi:10.1103/PhysRevLett.120.081801](#).
- [3] M. Aaboud, et al., Observation of electroweak production of a same-sign W boson pair in association with two jets in pp collisions at $\sqrt{s} = 13$ TeV with the ATLAS detector, *Phys. Rev. Lett.* 123 (16) (2019) 161801. [arXiv:1906.03203](#), [doi:10.1103/PhysRevLett.123.161801](#).
- [4] A. M. Sirunyan, et al., Measurements of production cross sections of polarized same-sign W boson pairs in association with two jets in proton-proton collisions at $\sqrt{s} = 13$ TeV [arXiv:2009.09429](#).
- [5] V. Khachatryan, et al., Study of vector boson scattering and search for new physics in events with two same-sign leptons and two jets, *Phys. Rev. Lett.* 114 (5) (2015) 051801. [arXiv:1410.6315](#), [doi:10.1103/PhysRevLett.114.051801](#).
- [6] M. Aaboud, et al., Search for anomalous electroweak production of WW/WZ in association with a high-mass dijet system in pp collisions at $\sqrt{s} = 8$ TeV with the ATLAS detector, *Phys. Rev. D* 95 (3) (2017) 032001. [arXiv:1609.05122](#), [doi:10.1103/PhysRevD.95.032001](#).
- [7] A. M. Sirunyan, et al., Search for anomalous electroweak production of vector boson pairs in association with two jets in proton-proton collisions at 13 TeV, *Phys. Lett. B* 798 (2019) 134985. [arXiv:1905.07445](#), [doi:10.1016/j.physletb.2019.134985](#).
- [8] A. M. Sirunyan, et al., Measurements of production cross sections of WZ and same-sign WW boson pairs in association with two jets in proton-proton collisions at $\sqrt{s} = 13$ TeV [arXiv:2005.01173](#).
- [9] Vector Boson Scattering prospective studies in the ZZ fully leptonic decay channel for the High-Luminosity and High-Energy LHC upgrades, Tech. Rep. CMS-PAS-FTR-18-014, CERN, Geneva (2018). URL <https://cds.cern.ch/record/2650915>
- [10] Vector Boson Scattering prospective studies in the ZZ fully leptonic decay channel for the High-Luminosity and High-Energy LHC upgrades, Tech. Rep. CMS-PAS-FTR-18-014, CERN, Geneva (12 2018).
- [11] P. Azzi, et al., Report from Working Group 1: Standard Model Physics at the HL-LHC and HE-LHC, Vol. 7, 2019, pp. 1–220. [arXiv:1902.04070](#), [doi:10.23731/CYRM-2019-007.1](#).
- [12] A. Ballestrero, et al., Precise predictions for same-sign W -boson scattering at the LHC, *Eur. Phys. J. C* 78 (8) (2018) 671. [arXiv:1803.07943](#), [doi:10.1140/epjc/s10052-018-6136-y](#).
- [13] S. Chatrchyan, et al., Measurement of the Polarization of W Bosons with Large Transverse Momenta in W +Jets Events at the LHC, *Phys. Rev. Lett.* 107 (2011) 021802. [arXiv:1104.3829](#), [doi:10.1103/PhysRevLett.107.021802](#).
- [14] G. Aad, et al., Measurement of the polarisation of W bosons produced with large transverse momentum in pp collisions at $\sqrt{s} = 7$ TeV with the ATLAS experiment, *Eur. Phys. J. C* 72 (2012) 2001. [arXiv:1203.2165](#), [doi:10.1140/epjc/s10052-012-2001-6](#).
- [15] M. Aaboud, et al., Measurement of the W boson polarisation in $t\bar{t}$ events from pp collisions at $\sqrt{s} = 8$ TeV in the lepton+jets channel with ATLAS [arXiv:1612.02577](#).
- [16] V. Khachatryan, et al., Measurement of the W boson helicity fractions in the decays of top quark pairs to lepton + jets final states produced in pp collisions at $\sqrt{s} = 8$ TeV, *Phys. Lett. B* 762 (2016) 512–534. [arXiv:1605.09047](#), [doi:10.1016/j.physletb.2016.10.007](#).
- [17] G. Aad, et al., Combination of the W boson polarization measurements in top quark decays using ATLAS and CMS data at $\sqrt{s} = 8$ TeV [arXiv:2005.03799](#).
- [18] G. Aad, et al., Measurement of the angular coefficients in Z -boson events using electron and muon pairs from data taken at $\sqrt{s} = 8$ TeV with the ATLAS detector, *JHEP* 08 (2016) 159. [arXiv:1606.00689](#), [doi:10.1007/JHEP08\(2016\)159](#).
- [19] V. Khachatryan, et al., Angular coefficients of Z bosons produced in pp collisions at $\sqrt{s} = 8$ TeV and decaying to $\mu^+\mu^-$ as a function of transverse momentum and rapidity, *Phys. Lett. B* 750 (2015) 154–175. [arXiv:1504.03512](#), [doi:10.1016/j.physletb.2015.08.061](#).
- [20] M. Aaboud, et al., Measurement of $W^\pm Z$ production cross sections and gauge boson polarisation in pp collisions at $\sqrt{s} = 13$ TeV with the ATLAS detector, *Eur. Phys. J. C* 79 (6) (2019) 535. [arXiv:1902.05759](#), [doi:10.1140/epjc/s10052-019-7027-6](#).
- [21] A. Ballestrero, E. Maina, G. Pelliccioli, W boson polarization in vector boson scattering at the LHC, *JHEP* 03 (2018) 170. [arXiv:1710.09339](#), [doi:10.1007/JHEP03\(2018\)170](#).
- [22] A. Ballestrero, E. Maina, G. Pelliccioli, Polarized vector bo-

- son scattering in the fully leptonic WZ and ZZ channels at the LHC, JHEP 09 (2019) 087. [arXiv:1907.04722](#), [doi:10.1007/JHEP09\(2019\)087](#).
- [23] G. Pelliccioli, Vector Boson Scattering at the LHC. A phenomenological study of massive gauge bosons polarization and precise predictions beyond leading order accuracy in the fully leptonic decay channel., Ph.D. thesis, Universita' Di Torino (2019).
- [24] X. Janssen, A. Mehta, Future perspectives for same-sign WW with Delphes, VBSCan@Helsinki meeting (February 2019).
- [25] A. Denner, S. Dittmaier, M. Roth, D. Wackeroth, Electroweak radiative corrections to $e^+e^- \rightarrow WW \rightarrow 4$ fermions in double-pole approximation: The RACONWW approach, Nucl. Phys. B587 (2000) 67–117. [arXiv:hep-ph/0006307](#), [doi:10.1016/S0550-3213\(00\)00511-3](#).
- [26] J. Baglio, L. D. Ninh, Polarization observables in WZ production at the 13 TeV LHC: Inclusive case, Commun. Phys. 30 (1) (2020) 35–47. [arXiv:1910.13746](#), [doi:10.15625/0868-3166/30/1/14461](#).
- [27] A. Ballestrero, A. Belhouari, G. Bevilacqua, V. Kashkan, E. Maina, PHANTOM: A Monte Carlo event generator for six parton final states at high energy colliders, Comput. Phys. Commun. 180 (2009) 401–417. [arXiv:0801.3359](#), [doi:10.1016/j.cpc.2008.10.005](#).
- [28] D. Buarque Franzosi, O. Mattelaer, R. Ruiz, S. Shil, Automated predictions from polarized matrix elements, JHEP 04 (2020) 082. [arXiv:1912.01725](#), [doi:10.1007/JHEP04\(2020\)082](#).
- [29] R. D. Ball, et al., Parton distributions for the LHC Run II, JHEP 04 (2015) 040. [arXiv:1410.8849](#), [doi:10.1007/JHEP04\(2015\)040](#).
- [30] A. Denner, S. Dittmaier, M. Roth, D. Wackeroth, Predictions for all processes $e^+e^- \rightarrow 4\text{fermions} + \gamma$, Nucl. Phys. B 560 (1999) 33–65. [arXiv:hep-ph/9904472](#), [doi:10.1016/S0550-3213\(99\)00437-X](#).
- [31] A. Denner, S. Dittmaier, M. Roth, L. Wieders, Electroweak corrections to charged-current $e^+e^- \rightarrow 4\text{fermion}$ processes: Technical details and further results, Nucl. Phys. B 724 (2005) 247–294, [Erratum: Nucl.Phys.B 854, 504–507 (2012)]. [arXiv:hep-ph/0505042](#), [doi:10.1016/j.nuclphysb.2011.09.001](#).
- [32] W. Stirling, E. Vryonidou, Electroweak gauge boson polarisation at the LHC, JHEP 07 (2012) 124. [arXiv:1204.6427](#), [doi:10.1007/JHEP07\(2012\)124](#).
- [33] A. Belyaev, D. Ross, What Does the CMS Measurement of W-polarization Tell Us about the Underlying Theory of the Coupling of W-Bosons to Matter?, JHEP 08 (2013) 120. [arXiv:1303.3297](#), [doi:10.1007/JHEP08\(2013\)120](#).
- [34] A. Denner, G. Pelliccioli, Polarized electroweak bosons in W^+W^- production at the LHC including NLO QCD effects, JHEP 09 (2020) 164. [arXiv:2006.14867](#), [doi:10.1007/JHEP09\(2020\)164](#).
- [35] E. Maina, Vector boson polarizations in the decay of the Standard Model Higgs, [arXiv:2007.12080](#).
- [36] K. Doroba, J. Kalinowski, J. Kuczmarski, S. Pokorski, J. Rosiek, M. Szleper, S. Tkaczyk, The $W_L W_L$ Scattering at the LHC: Improving the Selection Criteria, Phys. Rev. D 86 (2012) 036011. [arXiv:1201.2768](#), [doi:10.1103/PhysRevD.86.036011](#).